THE JOURNAL OF PHYSICAL CHEMISTRY C

Article

pubs.acs.org/JPCC

Effect of Disorder and Dipolar Interactions in Two-Dimensional Assemblies of Iron-Oxide Magnetic Nanoparticles

Guillaume Klughertz, Giovanni Manfredi,* Paul-Antoine Hervieux, Benoit P. Pichon, and Sylvie Begin-Colin

Institut de Physique et Chimie des Matériaux de Strasbourg, CNRS and Université de Strasbourg, 23 rue du Loess – BP 43, F - 67034 Strasbourg, France

ABSTRACT: We examine the magnetic properties of two-dimensional monolayers of iron-oxide magnetic nanoparticles arranged on a hexagonal lattice and interacting through magnetic dipole forces. Monte Carlo simulations are used to reconstruct the zero-field cooled magnetization curve, as well as other relevant quantities (Zeeman and dipolar energies). The blocking temperature is found to increase with shorter interparticle distance. The effect of structural disorder is studied by randomly removing some nanoparticles from their lattice sites. Surprisingly, it is found that disorder has little impact on the global magnetic structure of the sample. The numerical results are compared to existing experimental measurements.

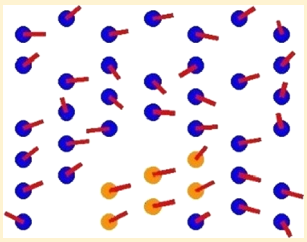

1. INTRODUCTION

Nanoparticle (NP) assemblies have attracted much interest for their potential applications in various fields, such as magnetic and magneto-resistive sensors.[1,2] In this context, the spatial arrangement of the NPs is a key element to control their collective properties through the fine-tuning of the dipolar interactions. However, assemblies of NPs usually form complex magnetic structures that are difficult to understand and to tailor at will. Significant progress has been made on the preparation of well-structured assemblies in recent years,[3] but their experimental preparation still faces several technical limitations which impede the high structuration of the assemblies. Although the influence of the structuring of NP assemblies on their collective magnetic properties has been widely reported,[4,5] the role of the interparticle distance on the dipolar interactions cannot be precisely assessed because it is directly related to the organization of the assembly.

On the other hand, the preparation of two-dimensional (2D) assemblies, such as monolayers with high topographical control, is well established.[6,7] In contrast to random assemblies such as powder, collective properties have been reported to be markedly enhanced by the shape anisotropy, which favors in-plane dipolar interactions.[8−13] The preparation of NP monolayers by the Langmuir−Blodgett technique with tunable interparticle distance (1−10 nm) confirmed that the blocking temperature behaves as a^{-3}, where a is the interparticle distance.[14] This scaling of the blocking temperature was also observed in solvents.[15] Although such NP assemblies display some local order,[16] the increase of the interparticle distance is generally accompanied by increasing disorder.[14] While disorder is acknowledged to be a critical parameter for the control of the collective properties of the NPs, it is difficult to study from a purely experimental point of view. Theoretical studies offer an interesting and complementary alternative to circumventing these limitations.[17−21] Monte Carlo simulations have confirmed that the blocking temperature is modified by the dipolar coupling strength[22−24] and scales as a^{-3}.[25,26] This effect was interpreted as an increase in the single-particle anisotropy barrier by the magnetic dipole−dipole interaction.

A computational approach also allows us to easily and accurately induce different kinds of disorder in the lattice. One can vary, for instance, the coverage of the nanoparticles over the monolayer:[26] while the total magnetization of the assembly strongly depends on this quantity, no significant difference was observed for the blocking temperature between 100% and 80% coverage. Alternatively, one can assign random positions to the NPs.[27,28] Brinis et al.[27] used a Monte Carlo technique to compute the magnetic susceptibility of a monolayer with a square unit cell but surprisingly noticed no significant difference between self-organized (ordered) and random assemblies when the anisotropy axes were in the plane of the monolayer. Using a dynamical approach based on the Landau−Lifshitz−Gilbert equation, Varòn et al.[28] observed that the magnetic structure induced by the dipolar interactions in a 2D lattice was roughly preserved under significant randomization of the NP positions and sizes. The only noticeable effect was a small reduction of the average magnetization. These numerical results were corroborated by experimental measurements.

Few studies have investigated the effect of disorder on the so-called zero-field cooled (ZFC) curve by means of both theoretical and experimental approaches.[26] ZFC is an experimental technique that allows one to determine the blocking temperature of an assembly of magnetic NPs. The sample is first cooled to a temperature of a few degrees Kelvin in the absence of any external magnetic field. If the anisotropy axes of the NPs are randomly oriented, then the total magnetization is roughly zero. Subsequently, a small magnetic field is applied and the temperature is gradually raised, allowing

Received: January 9, 2016
Revised: March 4, 2016

DOI: 10.1021/acs.jpcc.6b00254
J. Phys. Chem. C XXXX, XXX, XXX−XXX

the magnetic moments of the NPs to escape from the anisotropy energy barrier and to align with the magnetic field. Thus, the total magnetization increases and reaches a maximum at the blocking temperature T_{max}. For $T > T_{max}$, the magnetic moments fluctuate randomly (superparamagnetic regime) and the magnetization drops slowly to zero.

In ref 26, the authors induced the disorder by varying the coverage of a monolayer assembly. However, disorder can have different meanings for different investigators and can be set up in many ways. The most usual way consists in randomly shifting the positions of the NPs or inducing a distribution of sizes. However, to our knowledge, there exist no studies where the disorder is induced by removing some NPs while preserving the structure of the remaining ones. We believe this kind of disorder describes well our experimental samples where locally ordered domains exist on the scale of 20 nm.[16] Perturbing the positions of all nanoparticles would not be representative of such samples.

Herein, we report on the theoretical study of the collective properties of 2D assemblies of magnetic NPs, using a Monte Carlo technique where the random step is a rotation of the magnetic moment. To compare with the experimental results obtained earlier on Langmuir−Blodgett assemblies,[16,8,14] we consider iron-oxide NPs with a diameter of 10 nm distributed on a 2D hexagonal lattice. The dipolar interaction is computed exactly and thus depends critically on the spatial arrangement of the NPs in the monolayer. We will investigate the effect of disorder as a function of the interparticle distance and of the number of random vacancies in the lattice. The collective properties will be determined primarily from the temperature-dependent magnetization curves (ZFC curves) but also from the evolution of the various energy terms (dipolar and Zeeman energies) and the angular distribution of the magnetic moments of the NPs.

2. MODEL

We consider a monodisperse assembly of 49 iron-oxide magnetic NPs with diameter d = 10 nm, uniaxial anisotropy with constant $K = 2.82 \times 10^4$ J/m^3, and saturation magnetization $\mu_s = 2.5 \times 10^4\ \mu_B = 2.32 \times 10^{-19}$ J/T. This kind of NP does not exhibit more than one magnetic domain below a diameter of ∼30 nm,[29,30] and so we can work within the macrospin approximation. The NPs are spread over a hexagonal 2D lattice with lattice constant $a \geq d + 2.5$ nm. The anisotropy axes are initially oriented randomly in the $(\vec{e}_x, \vec{e}_y)$ plane defined by the layer. This configuration represents the state of the NP assembly after the ZFC phase.

A small external magnetic field $\overrightarrow{B_{ext}}$ of magnitude 7.5 mT is applied in the plane of the film. Then, the total energy of the ith NP is

$$E_i = E_{an}^i + E_Z^i + E_{dip}^i \tag{1}$$

where E_{an}^i is the anisotropy energy, E_Z^i is the Zeeman energy, and E_{dip}^i is the dipolar energy. Let us call φ_i the angle between the magnetic moment $\hat{m}_i = \overrightarrow{M_i}/\mu_s$ and the anisotropy axis, and $\vec{r}_i$ the position of the ith nanoparticle. The different energy terms can be written as follows

$$E_{an}^i = KV \sin^2 \varphi_i \tag{2}$$

$$E_Z^i = -\overrightarrow{M_i} \cdot \overrightarrow{B_{ext}} \tag{3}$$

$$E_{dip}^i = \sum_{j \neq i} \frac{\mu_0 \mu_s^2}{4\pi |\vec{r}_{ij}|^3} (\hat{m}_i \cdot \hat{m}_j - 3(\hat{m}_i \cdot \hat{r}_{ij})(\hat{m}_j \cdot \hat{r}_{ij})) \tag{4}$$

where $\vec{r}_{ij} = \vec{r}_i - \vec{r}_j$ denotes the center-to-center interparticle distance vector, and $\hat{r}_{ij} = \vec{r}_{ij}/|\vec{r}_{ij}|$ is the unit distance vector. The total energy is therefore determined by the relative orientation between the magnetic moments, as well as their own orientation with respect to the external magnetic field and their anisotropy axes. Because the distance between the NP surfaces is much larger than the range of the exchange interaction, we neglect the interaction between surface spins of neighboring NPs. The dipolar energy is computed exactly by evaluating the dipole−dipole interactions between all pairs of NPs. No periodic boundary conditions are assumed in our study.

We search for an equilibrium magnetic configuration at a given temperature; therefore, a Monte Carlo approach is the method of choice.[31,27,32,25] We used the Metropolis algorithm[33] to approach the Boltzmann distribution by seeking the most energetically favorable configuration under the effect of thermal agitation. A Monte Carlo step consists in randomly picking a NP, randomly modifying its magnetic moment, and then deciding whether to accept or reject this trial move on the basis of the energy difference $\Delta E = E_{trial} - E_t$, where E_t is the energy of the NP at the current time t. The trial state is accepted with a probability equal to unity if ΔE is negative, and it is picked in the distribution $\exp(\Delta E/k_B T)$ otherwise. At low temperatures, this algorithm tends to mostly accept lower free energy states, but the higher the temperature the higher the probability to make positive jumps in energy.

The random modification is in fact a rotation of the magnetic moment within a cone whose half-opening angle is temperature-dependent in order to maintain the Metropolis acceptance ratio at around 50%. The angle was determined empirically to fulfill this condition and reads as

$$\alpha[\text{rad}] = 0.031 T[\text{K}]^{0.585} + \frac{\pi}{800} \tag{5}$$

To reproduce a ZFC curve, we perform a Monte Carlo run for different temperatures starting from T_0 = 0 K, where each magnetic moment is initialized along its anisotropy axis. Then, the temperature is increased by steps of 5 K, that is, $T_{i+1} = T_i +$ 5 K, until T_{final} = 300 K. The magnetic configuration at T_i is taken as the starting point for the Monte Carlo algorithm at T_{i+1}. For each temperature, the code performs 10^4 Monte Carlo steps per NP to reach equilibrium, and only then it starts to compute the thermal averages of relevant variables, such as the in-plane magnetization of the sample, for another 5×10^5 Monte Carlo steps.

Each ZFC curve is obtained by averaging over 40 statistically independent realizations with different initial random orientations of the anisotropy axes. As the anisotropy axes are randomly oriented, the ensemble average of the magnetization at T = 0 K is approximately zero. At higher temperature, the thermal agitation becomes sufficient to unpin the magnetic moments from their anisotropy axes, and collective magnetic order is created by the combined action of the dipolar interaction and the external field. At even higher temperatures, the thermal energy becomes larger than any other magnetic energy, the NPs enter the superparamagnetic regime, and thus, the total magnetization tends to zero.

DOI: 10.1021/acs.jpcc.6b00254
J. Phys. Chem. C XXXX, XXX, XXX−XXX

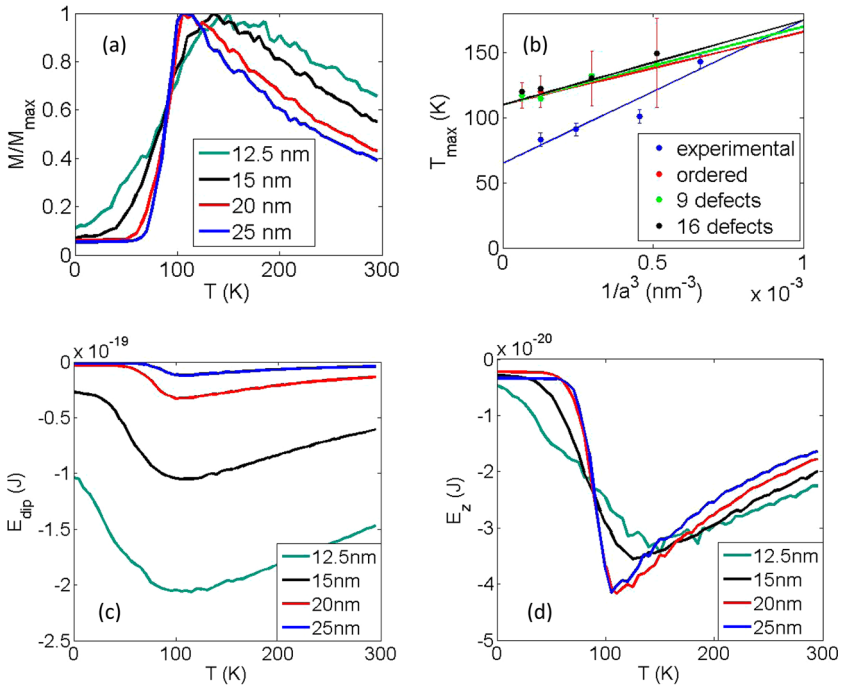

Figure 1. (a) ZFC curves of a hexagonal-ordered monolayer composed of 49 nanoparticles for different lattice parameters. We show the in-plane component of the total magnetization normalized to its maximum value. (b) Temperature values corresponding to the maximum of the ZFC curves as a function of the cube of the inverse interparticle distance for three sets of numerical simulations (red, green, and black) and one set of experimental data (blue).The straight lines are linear fits. (c) Dipolar energy as a function of the temperature for different lattice parameters. (d) Zeeman energy as a function of the temperature for different lattice parameters.

3. ORDERED HEXAGONAL PACKING

We first study a perfectly organized assembly of NPs. To reduce the density and thus decrease the strength of the dipolar interaction, one can increase the lattice parameter a to position the NPs farther away from each other. We will specifically study the cases where the center-to-center distance between nearest neighbors is 12.5, 15, 20, and 25 nm.

When varying the distance between lattice sites, we observe three effects on the ZFC curves (see Figure 1a):

- Increasing the interparticle distance leads to a smaller blocking temperature, which is expected[32,34,35,22,26,24] and has been observed experimentally.[14,36,37,10,19,9,38] The maximum of the magnetization curves ranges from 117 K for 25 nm to 142 K for 12.5 nm. Notice that there is not much difference above 20 nm, meaning that the dipolar interactions are very weak, and we recover the case of isolated NPs.
- The stronger the dipolar interaction the broader the maximum. This result can be explained as follows. For large interparticle distance, the NPs behave as if they were isolated, and because they are all identical, they respond in the same way to the temperature increase. In contrast, for closely packed assemblies, each NP experiences a slightly different environment, because it feels both the external magnetic field and the field generated by the other neighboring particles. This induces some dispersion in the effective blocking temperature of each individual NP, resulting in a broadening of the global curve.
- In the low-temperature range, the magnetization increases earlier and more slowly in the case of strong dipolar interactions. This means that the dipolar interactions facilitate the unpinning of the magnetic moment from its anisotropy axis and induce an in-plane magnetization more easily, as was already noticed.[27] In contrast, when the interactions are weaker and the NPs almost independent, the magnetic moments react as a whole in a more simultaneous way to the external field. This behavior is similar to what was observed experimentally in a study comparing 5 and 16 nm iron-oxide NPs.[8] The smaller (and thus weakly interacting) NPs displayed a narrower ZFC curve compared to the larger (and thus more strongly interacting) NPs. A steep increase has also been observed in field-dependent magnetization curves measured for iron-oxide NPs with similar sizes.[39]

Extracting the blocking temperature T_{max} from the data of Figure 1a, one can see that T_{max} scales as $1/a^3$ as expected from earlier results,[14] both experimental and theoretical. The corresponding standard deviation yields the error bars represented in the figure. When $a \rightarrow \infty$, one obtains the blocking temperature of an isolated NP, which is around 110 K according to the linear fit. The discrepancy with the experimental data of Fleutot et al.,[14] obtained for 10 nm sized iron-oxide NPs, is significant, especially in the weak-interaction regime. Such discrepancy may arise from a poor knowledge of the NP intrinsic parameters, for instance, the anisotropy constant or the magnetic moment. It may also be due to the magnetic contribution of the spins on the surface of the NPs, which was not considered in the present work. Indeed, magnetic NPs have been reported to exhibit surface spin-canting.[40] The difference between the theoretical and the experimental results would suggest that the magnetic contribution of the surface is influenced by the dipolar interactions. Indeed, the magnetic surface contribution of the

DOI: 10.1021/acs.jpcc.6b00254
J. Phys. Chem. C XXXX, XXX, XXX−XXX

NPs is more sensitive to dipolar interactions than the volume contribution.[41,42]

The $1/a^3$ scaling of T_{max} suggests a strong dependence on the dipolar interaction. However, Figure 1c shows that the minima of the dipolar energy, while drastically decreasing (in absolute value) with the interparticle distance, all occur at the same temperature (around 110 K). In contrast, the minima of the Zeeman energy perfectly match the maxima of the ZFC curves (Figure 1d) because, as the external magnetic field is constant, a minimum in the Zeeman energy can only be due to a maximum of the magnetization along $\overrightarrow{B_{ext}}$. Thus, the most favorable configuration of the magnetic moments with regard to the dipolar energy, which always happens around 110 K, does not necessarily correspond to the largest in-plane magnetization, which is realized at different temperatures between 110 and 150 K.

The behavior of the dipolar energy can be explained qualitatively as follows. Magnetic configurations that minimize the dipolar energy should be invariant with respect to distance scaling and only depend on the geometry of the assembly (here, a hexagonal lattice). This is because the corresponding magnetic order is given by particle−particle interactions that depend only on the distance and the angle between the magnetic moments. Thus, the temperature corresponding to these configurations should be independent of the interparticle distance, in agreement with Figure 1c (see also Figure 2). As a consequence, the position of the minimum of the dipolar energy only depends on the blocking temperature of isolated nanoparticles, which is around 110 K in our case, as can be extrapolated from Figure 1b in the limit $a \to \infty$.

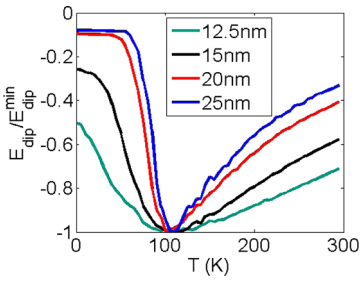

Figure 2. Normalized dipolar energy as a function of the temperature for different lattice parameters.

However, the robustness of these E_{dip}-minimizing configurations does depend on the distance. Indeed, for weaker dipolar interactions (larger distance), the dipolar energy tends more rapidly to zero when the temperature is raised, as can be seen from Figure 2. In contrast, for more closely packed assemblies, higher temperatures are required to counteract the magnetic order induced by the dipolar interactions. It appears that this order stems from the formation of local magnetic domains, such as rings or chains.

In summary, we can draw a global picture of the behavior of an assembly of magnetic NPs. At zero temperature, the magnetic moments are aligned with the anisotropy axes, which are randomly oriented thus yielding a vanishing total magnetization. Increasing the temperature, the magnetic moments overcome the anisotropy barrier and are free to form ordered magnetic domains. This occurs at the blocking temperature of an isolated NP (around 110 K in our example) and corresponds to a minimum of the dipolar energy. By further heating the sample, the domains are broken down and the magnetic moments can now orient themselves along the external field. This reorientation reaches a maximum between 110 and 150 K (blocking temperature T_{max}). For higher temperatures, thermal fluctuations induce complete disorder and the magnetization falls back to zero.

We can now understand why the position of T_{max} is shifted to higher temperatures for larger dipolar interactions. Indeed, for interacting NPs, one has to overcome two constraints to reach the maximum magnetization: first the anisotropy barrier, and then the local magnetic domains induced by the dipolar interactions. Breaking down these domains requires some additional energy, hence, a higher blocking temperature T_{max}.

4. EFFECT OF RANDOM DISORDER

We now introduce disorder in the sample by randomly removing some of the NPs from the lattice in order to reproduce the small defects observed experimentally in Langmuir−Blodgett monolayers.[8,14] These films exhibit local hexagonal arrangement, but the spatial correlation length is only approximately 20 nm,[16] which is about twice the distance between two NPs. Larger scale order is prevented by holes (defects), which we model numerically as empty sites on the lattice. Each of the 40 realizations involves a different random distribution of defects among the available lattice sites. We remove 9 (18%) or 16 (33%) NPs among the 49 available sites. The spatial density is therefore considerably altered.

The effect of adding random empty sites is counterintuitive. Whatever the lattice parameter, removing even 33% of the NPs does not seem to significantly alter the blocking temperature in the magnetization curve (Figure 3a). This is somewhat puzzling because a reduced density should lower the strength of the dipolar interactions and therefore lead to a smaller blocking temperature, as in Figure 1a. However, our observation is in line with the findings of Brinis et al.,[27] who also did not observe any visible influence of randomness on the peak position. Our approach is different in three respects: (1) The easy axes have random directions, whereas for Brinis et al.[27] they all have the same direction in the plane; (2) our random trial move is a rotation of the magnetic moment within a cone, whereas theirs is a single spin flip; (3) the randomness is not introduced in the same way: we take a perfectly organized lattice and remove some NPs, whereas they assigned random positions to all the NPs. In doing so, we preserve the local order by keeping small structurally ordered domains. Despite these differences, we note the same absence of significant effect of structural disorder on the blocking temperature, as was also observed in three-dimensional supracrystals[43] and monolayers.[26]

The dipolar energy (Figure 3c) shows no variation as to the position of its minimum, but its decreasing tail seems affected by the addition of defects. This is even more visible when the lattice parameter a is large, that is, in the weak-interaction regime. One can also see this effect for a 12.5 nm lattice parameter but to a lesser extent. The Zeeman energy (not shown) displays no variation with the number of defects, either regarding the blocking temperature or the tail of the curve.

The fact that the addition of disorder has little or no influence on the magnetization curves may be due to a lowering of magnetic frustration. When removing some nanoparticles, there are fewer constraints on the remaining magnetic moments, which can more easily form small local domains where the magnetic order is determined by the dipolar interaction. These magnetic structures, which are harder to

DOI: 10.1021/acs.jpcc.6b00254
J. Phys. Chem. C XXXX, XXX, XXX−XXX

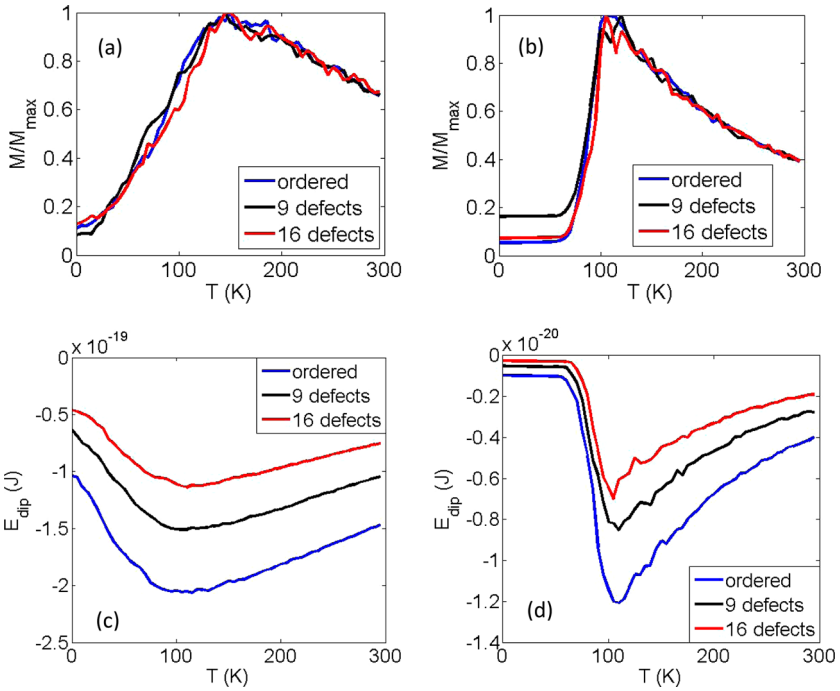

Figure 3. Top: ZFC curves (total magnetization versus temperature) of a monolayer of 49 (blue), 40 (black), and 33 (red) nanoparticles allocated among 49 lattice sites for lattice parameters (a) a = 12.5 nm and (b) a = 25 nm. Bottom: Dipolar energy as a function of the temperature for the same systems, with lattice parameters (c) a = 12.5 nm or (d) a = 25 nm.

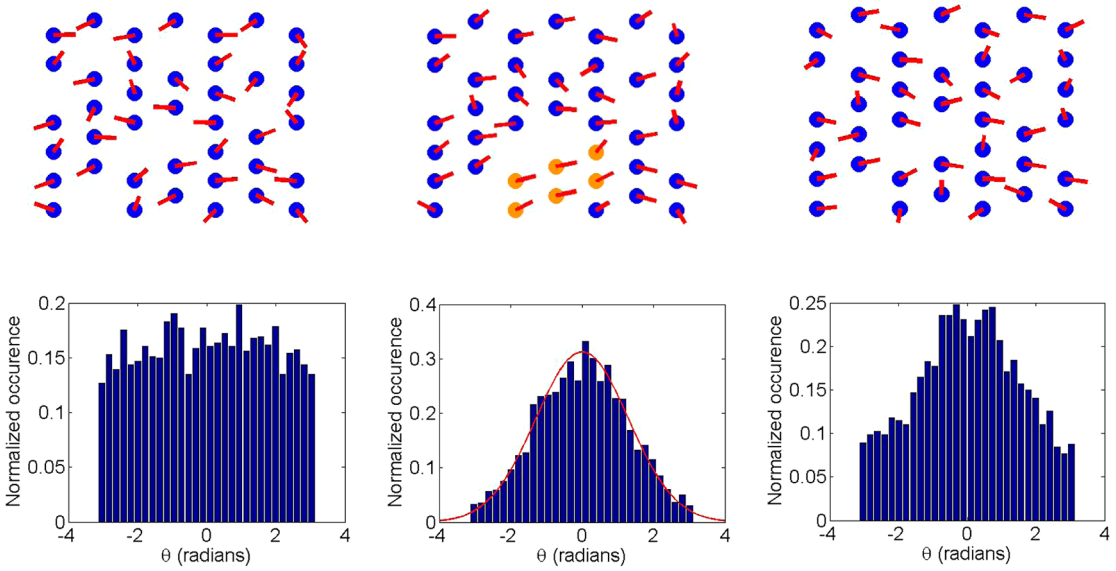

Figure 4. Top panels: Map of an ensemble of 40 nanoparticles separated by a distance of 15 nm and presenting 9 defects, taken at T = 0 K (left), T = 125 K (middle), and T = 295 K (right). In the middle plot, an example of magnetic domain is highlighted in yellow. Bottom panels: Corresponding angular distributions averaged over all realizations. The red line is a Gaussian fit.

demagnetize for the temperature and the external field, may thus compensate for the lower density.

In Figure 4, we show a map of the sample, picturing the positions of the NPs and the orientations of their magnetic moments. Here, the external magnetic field is applied along the $\vec{e}_x$ direction, and θ_i is defined, for each NP, as the angle between its magnetic moment and the direction of the field.

We also plot in Figure 4 (bottom panels) the distribution of the angles θ_i, averaged over all realizations with the same number of defects. At T = 0 K, the magnetic moments are randomly oriented, resulting in a uniform angular distribution. The average magnetization therefore approaches zero (left panels on Figure 4). Then, at a temperature close to the maximum of the ZFC curves (T = 125 K, middle plots), the angular distribution tightens around zero. Most of the moments align with the field and some even form chainlike structures covering up to six nanoparticles (highlighted in yellow in the figure). Finally, at T = 295 K (right plots), most of the dipoles are still oriented along the external field, but the distribution flattens and widens.

Using a Gaussian function to fit the angular distributions of Figure 4, we can retrieve the standard deviation, which is shown

DOI: 10.1021/acs.jpcc.6b00254
J. Phys. Chem. C XXXX, XXX, XXX−XXX

Table 1. Standard Deviation of the Angular Distribution at T = 125 K, for Different Values of the Lattice Parameter and Different Numbers of Defects

	12.5 nm	15 nm	20 nm	25 nm
no defects	2.37 ± 0.05	2.17 ± 0.01	2.09 ± 0.01	2.17 ± 0.02
9 defects	2.52 ± 0.08	2.25 ± 0.004	2.11 ± 0.1	2.16 ± 0.26
16 defects	2.36 ± 0.11	2.29 ± 0.01	2.30 ± 0.1	2.27 ± 0.12

in Table 1 for different lattice parameters and numbers of defects. In the case of assemblies with no defects, stronger dipolar interactions result in a broader angular distribution, that is, the magnetic moments tend to be less aligned with the external field at the magnetization peak. Such broadening of the angular distribution can be correlated with the broadening of the magnetization curve and the dipolar energy (Figure 1a and c) and may be ascribed to the strong magnetic frustration arising from the 2D character of the assembly. In contrast, the standard deviation tends to decrease for larger interparticle distance, which means that the system tends to favor a unidirectional orientation of magnetic moments. Such behavior is particularly pronounced in the case of assemblies containing 9 defects. In contrast, samples with 16 defects exhibit rather similar values of the standard deviation, because of weak dipolar interactions.

Finally, with the exception of the strong interaction regime, a broadening of the angular distribution is observed when the number of defects increases, whatever the original center-to-center distance. This is similar to what was observed earlier in a system without defects: the dipolar interactions broaden the angular distribution (and the ZFC curve, see Figure 1a) because they slightly randomize the local environment of each NP. Here, the same effect is achieved by the introduction of random defects.

5. CONCLUSION

In this work, we studied the influence of dipolar interactions and structural disorder on the ZFC curves of an NP monolayer. The NPs are located on the sites of a lattice with hexagonal unit cell and interact via long-range dipolar forces. Their anisotropy axes are randomly distributed in the plane of the layer. We used a Monte Carlo method based on the Metropolis algorithm to find the equilibrium magnetic configuration at a given temperature, induced by the combined action of the dipolar interactions, the anisotropy field, and the external magnetic field. This procedure allowed us to reconstruct numerically the zero-field cooled curves that we later compared to existing experimental results. In the case of ordered monolayers, we found a good agreement between experimental and numerical data and observed an increase of the blocking temperature when the interparticle distance is lowered. We also found that the minimum in dipolar energy is determined by the properties of isolated NPs, although the interparticle distance affects the rate at which the dipolar energy goes to zero at high temperatures.

These findings indicate that the ZFC curve for interacting NPs results from two effects: first, at relatively low temperature, the magnetic moments overcome the single-particle anisotropy barrier and form small magnetic domains; then, at higher temperature, thermal effects destroy these domains so that the magnetic moments are able to align with the external field. This two-step mechanism explains the increase of the blocking temperature with shorter interparticle distance.

We then introduced disorder into the system by removing some NPs from their lattice sites: this procedure preserves local order on the scale of 20 nm, as in the experiments. We found that there is no major change in the shape of the ZFC curves even after removing 33% of the NPs. These results show that the dipolar interactions predominate over disorder: even though only a fraction of the NPs remain, they are still able to induce strong collective properties. This observation corroborates earlier studies that examined the effect of disorder in monolayers, although in our case the disorder was created in a very different way. We explained this behavior by noting that removing some of the NPs lowers the magnetic frustration and facilitates the formation of magnetic domains that are energetically favorable for the dipolar interaction. These domains are more resistant to the temperature and compensate for the loss in coverage (lower NP density).

AUTHOR INFORMATION

Corresponding Author

*E-mail: giovanni.manfredi@ipcms.unistra.fr.

Notes

The authors declare no competing financial interest.

ACKNOWLEDGMENTS

We acknowledge the financial support of the French Agence Nationale de la Recherche through the project Equipex UNION, grant n° ANR-10-EQPX-52.

REFERENCES

(1) Gutfleisch, O.; Willard, M. A.; Brück, E.; Chen, C. H.; Sankar, S. G.; Liu, J. P. *Adv. Mater.* **2011**, *23*, 821.
(2) Terris, B. D.; Thomson, T. *J. Phys. D: Appl. Phys.* **2005**, *38*, R199.
(3) Bellido, E.; Domingo, N.; Ojea-Jimenez, I.; Ruiz-Molina, D. *Small* **2012**, *8*, 1465.
(4) Dai, Q.; Nelson, A. *Chem. Soc. Rev.* **2010**, *39*, 4057.
(5) Neouze, M.-A. J. *J. Mater. Sci.* **2013**, *48*, 7321.
(6) Kinge, S.; Crego-Calama, M.; Reinhoudt, D. N. *ChemPhysChem* **2008**, *9*, 20.
(7) Tao, A. R.; Huang, J.; Yang, P. *Acc. Chem. Res.* **2008**, *41*, 1662.
(8) Pauly, M.; Pichon, B. P.; Panissod, P.; Fleutot, S.; Rodriguez, P.; Drillon, M.; Begin-Colin, S. *J. Mater. Chem.* **2012**, *22*, 6343.
(9) Poddar, P.; Morales, M. B.; Frey, N. A.; Morrison, S. A.; Carpenter, E. E.; Srikanth, H. *J. Appl. Phys.* **2008**, *104*, 063901.
(10) Poddar, P.; Telem-Shafir, T.; Fried, T.; Markovich, G. *Phys. Rev. B: Condens. Matter Mater. Phys.* **2002**, *66*, 060403.
(11) Zhang, H.; Bao, N.; Yuan, D.; Ding, J. *Phys. Chem. Chem. Phys.* **2013**, *15*, 14689.
(12) Braun, F.-K.; Sievers, S.; Albrecht, M.; Siegner, U.; Landfester, K.; Holzapfel, V. *J. Magn. Magn. Mater.* **2009**, *321*, 3719.
(13) Faure, B.; Wetterskog, E.; Gunnarsson, K.; Josten, E.; Hermann, R. P.; Bruckel, T.; Andreasen, J. W.; Meneau, F.; Meyer, M.; Lyubartsev, A.; Bergstrom, L.; Salazar-Alvarez, G.; Svedlindh, P. *Nanoscale* **2013**, *5*, 953.
(14) Fleutot, S.; Nealon, G. L.; Pauly, M.; Pichon, B. P.; Leuvrey, C.; Drillon, M.; Gallani, J.-L.; Guillon, D.; Donnio, B.; Begin-Colin, S. *Nanoscale* **2013**, *5*, 1507.

DOI: 10.1021/acs.jpcc.6b00254
J. Phys. Chem. C XXXX, XXX, XXX−XXX

(15) Bae, C. J.; Angappane, S.; Park, J.-G.; Lee, Y.; Lee, J.; An, K.; Hyeon, T. *Appl. Phys. Lett.* **2007**, *91*, 102502.
(16) Pauly, M.; Pichon, B. P.; Albouy, P.-A.; Fleutot, S.; Leuvrey, C.; Trassin, M.; Gallani, J.-L.; Begin-Colin, S. *J. Mater. Chem.* **2011**, *21*, 16018.
(17) Vargas, J. M.; Nunes, W. C.; Socolovsky, L. M.; Knobel, M.; Zanchet, D. *Phys. Rev. B: Condens. Matter Mater. Phys.* **2005**, *72*, 184428.
(18) Russier, V. *J. Appl. Phys.* **2001**, *89*, 1287.
(19) Knobel, M.; Nunes, W. C.; Winnischofer, H.; Rocha, T. C. R.; Socolovsky, L. M.; Mayorga, C. L.; Zanchet, D. *J. Non-Cryst. Solids* **2007**, *353*, 743.
(20) Russier, V.; Petit, C.; Legrand, J.; Pileni, M. P. *Phys. Rev. B: Condens. Matter Mater. Phys.* **2000**, *62*, 3910.
(21) Georgescu, M.; Viota, J. L.; Klokkenburg, M.; Erné, B. H.; Vanmaekelbergh, D.; Zeijlmans van Emmichoven, P. A. *Phys. Rev. B: Condens. Matter Mater. Phys.* **2008**, *77*, 024423.
(22) Kechrakos, D.; Trohidou, K. N. *Phys. Rev. B: Condens. Matter Mater. Phys.* **1998**, *58*, 12169.
(23) Azeggagh, M.; Kachkachi, H. *Phys. Rev. B: Condens. Matter Mater. Phys.* **2007**, *75*, 174410.
(24) Figueiredo, W.; Schwarzacher, W. *Phys. Rev. B: Condens. Matter Mater. Phys.* **2008**, *77*, 104419.
(25) Kechrakos, D.; Trohidou, K. N. *J. Nanosci. Nanotechnol.* **2008**, *8* (6), 2929−2943.
(26) Kechrakos, D.; Trohidou, K. N. *Appl. Phys. Lett.* **2002**, *81*, 4574−4576.
(27) Brinis, D.; Laggoun, A.; Ledue, D.; Patte, R. *J. Appl. Phys.* **2014**, *115*, 173906.
(28) Varón, M.; Beleggia, M.; Kasama, T.; Harrison, R. J.; Dunin-Borkowski, R. E. *Sci. Rep.* **2013**, *3*, 1234.
(29) Gubin, S. P. *Magnetic Nanoparticles*; Wiley-VCH: Weinheim, Germany, 2009.
(30) Wernsdorfer, W.; Orozco, E. B.; Hasselbach, K.; Benoit, A.; Barbara, B.; Demoncy, N.; Loiseau, A.; Pascard, H.; Mailly, D. *Phys. Rev. Lett.* **1997**, *78*, 1791.
(31) Andersson, J. O.; Djurberg, C.; Jonsson, T.; Svedlindh, P.; Nordblad, P. *Phys. Rev. B: Condens. Matter Mater. Phys.* **1997**, *56*, 13983.
(32) Garcia-Otero, J.; Porto, M.; Rivas, J.; Bunde, A. *Phys. Rev. Lett.* **2000**, *84*, 167.
(33) Metropolis, N.; Rosenbluth, A. W.; Rosenbluth, M. N.; Teller, A. H.; Teller, E. *J. Chem. Phys.* **1953**, *21* (6), 1087−1092.
(34) Dormann, J. L.; Bessais, L.; Fiorani, D. *J. Phys. C: Solid State Phys.* **1988**, *21*, 2015−2034.
(35) Dormann, J. L.; Fiorani, D.; Tronc, E. *Adv. Chem. Phys.* **1997**, *98*, 283−494.
(36) Pichon, B. P.; Louet, P.; Felix, O.; Drillon, M.; Begin-Colin, S.; Decher, G. *Chem. Mater.* **2011**, *23*, 3668−3675.
(37) Toulemon, D.; Pichon, B. P.; Cattoen, X.; Wong Chi Man, M.; Begin-Colin, S. *Chem. Commun.* **2011**, *47*, 11954−11956.
(38) Petit, C.; Russier, V.; Pileni, M. P. *J. Phys. Chem. B* **2003**, *107*, 10333.
(39) Pichon, B. P.; Pauly, M.; Marie, P.; Leuvrey, C.; Begin-Colin, S. *Langmuir* **2011**, *27*, 6235.
(40) Baaziz, W.; Pichon, B. P.; Fleutot, S.; Liu, Y.; Lefevre, C.; Greneche, J.-M. *J. Phys. Chem. C* **2014**, *118*, 3795.
(41) Kostopoulou, A.; Brintakis, K.; Vasilakaki, M.; Trohidou, K. N.; Douvalis, A. P.; Lascialfari, A.; Manna, L.; Lappas, A. *Nanoscale* **2014**, *6*, 3764.
(42) Sabsabi, Z.; Vernay, F.; Iglesias, O.; Kachkachi, H. *Phys. Rev. B: Condens. Matter Mater. Phys.* **2013**, *88*, 104424.
(43) Pileni, M.-P. *Acc. Chem. Res.* **2007**, *40*, 685.

DOI: 10.1021/acs.jpcc.6b00254
J. Phys. Chem. C XXXX, XXX, XXX−XXX